Articles

Syntheses, Structures, and Thermal Behavior of Cu(hfacac) Complexes Derived from Ethanolamines

Jirí Pinkas,[†] John C. Huffman,[‡] John C. Bollinger,[‡] William E. Streib,[‡] David V. Baxter,*[,§] Malcolm H. Chisholm,*[,†] and Kenneth G. Caulton*[,†]

Departments of Chemistry and Physics and Molecular Structure Center, Indiana University, Bloomington, Indiana 47405-4001

Received April 4, 1996[⊗]

A series of novel precursors for MOCVD of metallic copper have been synthesized and structurally characterized. These precursors are composed of $Cu(hfacac)_2$, which serves as a volatile source of Cu, and amino alcohols, which act as reductants and anchor firmly to the copper center through the amine unit. In some cases, a proton transfer from the coordinated alcohol to the hfacac ligand results in the formation of an alkoxide unit and the release of the free Hhfacac. Metallic copper films can be deposited by MOCVD at 300 °C without any external reductant. Crystal data: $Cu(hfacac)_2 \cdot C_7H_8$ (−103 °C), $a = 6.510(6)$ Å, $b = 8.594(7)$ Å, $c = 18.478(15)$ Å, orthorhombic space group *Pmnn*, $Z = 2$; $Cu(hfacac)_2(H_2NCH_2CH_2OH)$ (−158 °C), $a = 13.145(1)$ Å, $b = 13.418(1)$ Å, $c = 11.245(1)$ Å, $\alpha = 110.39(1)°$, $\beta = 99.12(1)°$, $\gamma = 97.90(1)°$, triclinic space group $P\bar{1}$, $Z = 4$; $[Cu(hfacac)(Me_2NCH_2CH_2O)]_2$ (−153 °C), $a = 9.259(2)$ Å, $b = 12.011(3)$ Å, $c = 6.304(1)$ Å, $\alpha = 91.19(1)°$, $\beta = 106.66(1)°$, $\gamma = 74.83(1)°$, triclinic space group $P\bar{1}$, $Z = 1$; $Cu(hfacac)[N(CH_2CH_2OH)_2(CH_2CH_2O)] \cdot MeOH$ (−168 °C), $a = 10.075(4)$ Å, $b = 8.611(4)$ Å, $c = 19.259(9)$ Å, $\beta = 99.82(2)°$, monoclinic space group $P2_1/m$, $Z = 4$.

Introduction

We are interested in understanding the chemical processes involved in chemical vapor deposition (CVD) of copper and copper oxide films from $Cu(hfacac)_2$ (hfacac = hexafluoroacetylacetonate), **1**. In our previous studies we found that H_2O facilitates the release of the hfacac ligand from the $Cu(hfacac)_2(H_2O)$, **2**, precursor by a proton transfer.[1] Other workers found an addition of alcohols such as ethanol and 2-propanol into the CVD system to be beneficial for the reduction of the precursor to copper metal.[2−6] Unfortunately, both water and alcohols form adducts with $Cu(hfacac)_2$ that are unstable at a reduced pressure in the gas phase. Therefore, an excess of these coreactants has to be added for the reaction to take place. On the other hand, ammonia forms a sublimable complex $Cu(hfacac)_2(NH_3)$, **3**, which does not lose the NH_3 ligand under CVD conditions.[7]

The combination of an anchoring ability of amino ligands with a ligand-releasing and reducing action of alcohols led us to design and synthesize a new class of potential precursors

Chart 1

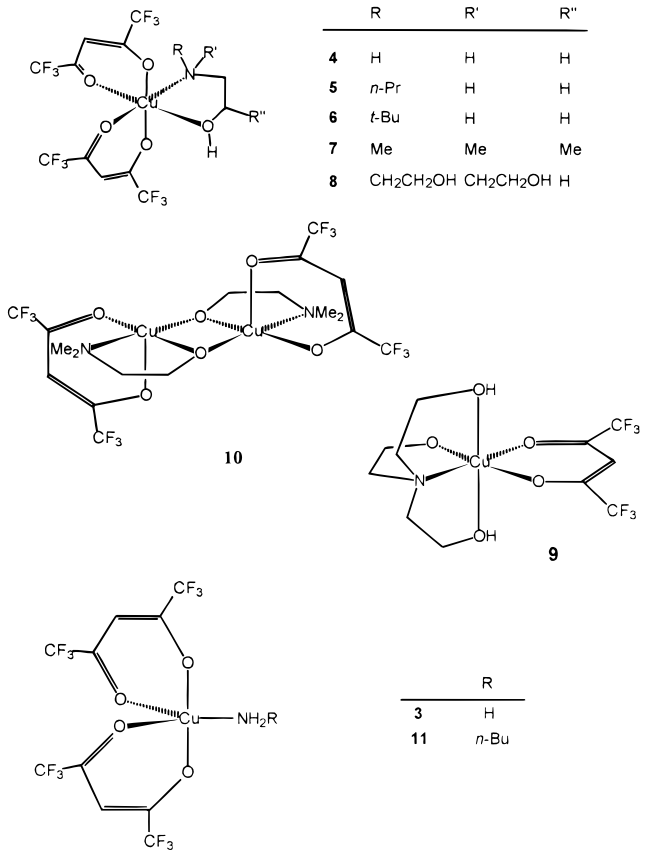

4−**11** (see Chart 1) whose structural and chemical characterization and thermal behavior are reported here.

[†] Department of Chemistry.
[‡] Molecular Structure Center.
[§] Department of Physics.
[⊗] Abstract published in *Advance ACS Abstracts,* June 15, 1997.

(1) Pinkas, J.; Huffman, J. C.; Baxter, D. V.; Chisholm, M. H.; Caulton, K. G. *Chem. Mater.* **1995**, *7*, 1589.
(2) Jones, C. R.; Houle, F. A.; Kovac, C. A.; Baum, T. H. *Appl. Phys. Lett.* **1985**, *46*, 97.
(3) Houle, F. A.; Wilson, R. J.; Baum, T. H. *J. Vac. Sci. Technol. A* **1986**, *4*, 2452.
(4) Pilkington, R. D.; Jones, P. A.; Ahmed, W.; Tomlinson, R. D.; Hill, A. E.; Smith, J. J.; Nuttall, R. *J. Phys. IV* **1991**, *C2*, 263.
(5) Zheng, B.; Eisenbraun, E. T.; Liu, J.; Kaloyeros, A. E. *Appl. Phys. Lett.* **1992**, *61*, 2175.
(6) Doppelt, P.; Baum, T. H. *MRS Bull.* **1994**, *19*, 41.
(7) Pinkas, J.; Huffman, J. C.; Chisholm, M. H.; Caulton, K. G. *Inorg. Chem.* **1995**, *34*, 5314.

S0020-1669(96)00370-9 CCC: $14.00

Two different reactivity patterns were observed for the series of substituted ethanolamines. 2-(Dimethylamino)ethanol and triethanolamine are capable of protonating and liberating one of the hfacac ligands in **1** and thereby forming Cu−O (alkoxide) bonds, while the rest of the examined ethanolamines form 1:1 complexes with **1**.

These new precursors are sublimable and carry, firmly attached through their amino functionality, 2 reducing equiv in their alcohol groups which, together with the reducing ability of the hfacac ligand,[1] should be sufficient for the reduction of Cu^{2+} to Cu^0, even in the absence of an external reductant such as H_2 gas. The reducing function of alcohols was demonstrated previously by depositing copper metal from **1**·^{i}PrOH at 160 °C using an excess of 2-propanol in nitrogen gas at 1 atm.[8] Acetone was detected as the oxidation product. Furthermore, the reducing action of alkoxides which are presumably intermediates in these reactions was utilized to obtain metallic copper by pyrolysis of **12** at 300 °C under nitrogen at ambient pressure.[9] Similarly, pure copper films were grown by CVD from **13**, and 2-(dimethylamino)ethanal was identified among the reaction products by IR spectroscopy.[10]

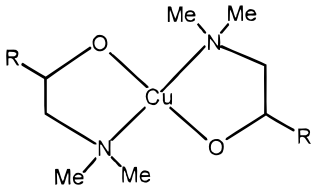

	R
12	Me
13	H

Experimental Section

Ethanolamines and $Cu(hfacac)_2(H_2O)$ were supplied by Aldrich. Dark blue crystalline anhydrous $Cu(hfacac)_2$ was prepared by a slow double sublimation of the hydrate at 60−70 °C and 10^{-2} Torr; mp 98−99 °C.[11] Both MS and IR spectra agreed with literature data.[12−14] The OH stretching vibrations were absent in the latter. Anhydrous $Cu(hfacac)_2$ was handled in a He-filled drybox. $Cu(hfacac)_2(NH_3)$ was prepared according to our procedure published previously.[7]

^{1}H (500.138 MHz) and ^{13}C (125.759 MHz) NMR spectra were recorded on a Bruker AM500 instrument at room temperature and were referenced to the corresponding TMS signals. ^{19}F (339.721 MHz) NMR spectra were obtained on a Nicolet NT360 instrument and referenced to the signal of CF_3COOH at −78.5 ppm in a particular deuterated solvent. Toluene-d_8, CD_2Cl_2, $CDCl_3$, and acetone-d_6 were used as internal locks. IR spectra were acquired on a Nicolet 510P FTIR spectrometer (4000−400 cm^{-1}) in KBr pellets. X-ray powder diffraction studies (XPD) were performed on a Scintag XDS 2000 powder diffractometer equipped with a Cu source (λ = 1.540 60 Å). A power of 1.4 kW and a continuous scan rate of 0.1°/min were used.

Mass spectra were run on a Kratos MS-80RFA high-resolution instrument using the EI mode at 30 and 80 eV, the CI mode with CH_4 ionizing gas, and the FAB mode with an NBA matrix.

Elemental analysis was performed by Atlantic Microlab. Melting points were measured in sealed capillaries and are uncorrected.

General Procedure for Syntheses of 4−7. Compound **1** (3.02−3.73 mmol) was dissolved in 50 mL of MeOH, and ethanolamines (3.14−3.91 mmol) in 10 mL of MeOH were added dropwise with stirring. The solution color changed from light to dark green, and a small exothermic effect was observed. The reaction solution was stirred at room temperature for 2 h.

Isolation and Characterization of the Individual Compounds. Compound 4. All volatile components were removed under vacuum, and the green solid was sublimed at 75−95 °C and 0.01 Torr, giving 67% **4**: mp 154.0−155.0 °C; IR (KBr pellet, 4000−400 cm^{-1}) ν 3484 s, br (ν(OH)), 3355 m (ν_{as}(NH)), 3282 s (ν_s(NH)), 3174 w, 3144 w (ν(CH)), 2962 w, 2909 w, 1670 sh, 1648 vs, 1610 w, 1597 m, 1559 m, 1532 s, 1484 s, 1456 vs, 1386 w, 1353 w, 1337 w, 1322 w, 1260 vs, 1220 vs, 1207 vs, 1149 vs, 1109 w, 1087 m, 1063 s, 1027 m, 994 w, 876 w, 802 s, 769 w, 745 w, 677 s, 670 s, 589 s, 578 sh, 523 w.

Compound 5. Volatile components were removed under vacuum, giving a green oil which partially crystallized within a week. The crystalline fraction was isiolated and sublimed at 75 °C and 0.01 Torr, giving 31% **5**: mp 74−78 °C; IR (KBr pellet, 4000−400 cm^{-1}) ν 3513 m, br (ν(OH)), 3284 w (ν(NH)), 3144 w (ν(CH)), 2977 m, 2953 w, 2886 m, 1673 m, 1646 s, 1603 w, 1558 s, 1552 s, 1530 m, 1489 s, 1486 s, 1458 s, 1433 w, 1353 w, 1257 vs, 1204 vs, 1150 vs, 1107 w, 1086 s, 1054 m, 1033 m, 1009 s, 941 m, 906 w, 895 m, 801 s, 794 s, 760 m, 746 m, 676 vs, 671 vs, 588 s, 529 m.

Compound 6. A green solid obtained after removing all volatile components was sublimed at 130 °C and 0.01 Torr, affording 68% **6**: mp 139−142 °C; IR (KBr pellet, 4000−400 cm^{-1}) ν 3249 w, 3228 w (ν(NH)), 3145 w (ν(CH)), 2991 m, 2917 w, 2872 m, 2789 w, br, 1666 m, 1647 vs, 1595 m, 1561 m, 1531 m, 1495 sh, 1477 s, 1452 m, 1410 m, 1386 m, 1377 w, 1355 w, 1344 w, 1255 vs, 1214 vs, 1203 vs, 1147 vs, 1137 sh, 1107 m, 1083 w, 1018 w, 939 w, 912 m, 800 s, 791 m, 764 m, 747 m, 721 w, 679 s, 659 s, 592 s, 575 m, 530 m.

Compound 7. All volatile components were removed under vacuum, yielding a dark green, oily liquid which partially crystallized. The crystalline portion was isolated and sublimed at 55−60 °C and 0.01 Torr, yielding 52% **7**: mp 56−58 °C; IR (KBr pellets, 4000−400 cm^{-1}) ν 3227 m, br (ν(OH)), 3143 w (ν(CH)), 3025 w, 2993 w, 2940 w, 2856 w, 1677 m, 1657 s, 1598 w, 1562 m, 1552 m, 1528 s, 1496 m, 1477 m, 1468 m, 1445 w, 1342 m, 1260 vs, 1218 s, 1208 s, 1185 vs, 1144 vs, 1136 vs, 1079 s, 1016 m, 1008 m, 943 m, 856 m, 837 w, 805 s, 798 s, 771 w, 744 m, 669 s, 664 m, 587 m, 578 w, 526 w.

Compound 8. Compound **1** (9.56 g, 20.0 mmol) was dissolved in 50 mL of dry toluene, and triethanolamine (2.98 g, 20.0 mmol) in 15 mL of THF was added dropwise with stirring. The dark green color turned pale, and a precipitate appeared. The reaction mixture was further stirred for 4 h, and half of the solvent was removed under vacuum. Filtration followed by washing with 40 mL of pentane and drying in vacuum afforded 11.03 g (88.0%) of **8**: mp 121−123 °C; IR (KBr pellet, 4000−400 cm^{-1}) ν 3359 m (ν(OH)), 3147 w (ν(CH)), 2992 w, 2919 w, 2787 w, 1665 m, 1649 s, 1536 vs, 1514 m, 1470 m, 1456 s, 1354 w, 1332 w, 1258 vs, 1210 vs, 1148 vs, 1074 m, 1038 w, 905 m, 804 m, 796 s, 747 w, 677 s, 590 m, 577 m, 530 w.

Compound 9. To compound **1** (1.686 g, 3.530 mmol) in 10 mL of MeOH was added dropwise with stirring triethanolamine (0.53 g, 3.5 mmol) in 7 mL of MeOH. After 15 min of stirring at room temperature, a green precipitate appeared. Filtration and drying in vacuum afforded 45% **9**: mp 160−162 °C dec; IR (KBr pellet, 4000−400 cm^{-1}) ν 3428 m, br, 3101 w, br, 2994 w, 2973 w, 2899 m, br, 2708 m, br, 1669 sh, 1651 vs, 1591 w, 1555 s, 1527 m, 1507 w, 1483 m, 1455 m, 1405 w, 1387 vw, 1372 w, 1350 w, 1260 vs, 1219 vs, 1192 s, 1147 sh, 1142 vs, 1108 m, 1099 m, 1086 m, 1062 m, 1030 w, 1016 w, 928 w, 908 s, 898 w, 812 w, 793 s, 761 w, 744 w, 675 s, 662 w, 615 w, 589 m, 564 w, 529 w, 496 m.

Compound 10. Compound **1** (2.99 g, 6.27 mmol) was dissolved in 10 mL of MeOH, and 2-(dimethylamino)ethanol (0.56 g, 6.28 mmol) in 5 mL of MeOH was added dropwise with stirring. The light green color changed to dark green, and a precipitate appeared. The solid was removed by filtration, and an additional crop was obtained by storing the mother liquor at −20 °C. The combined product fractions were sublimed at 80−100 °C and 0.01 Torr, providing a 92% yield of **10**: mp 194−195 °C; IR (KBr pellet, 4000−400 cm^{-1}) ν 3140 w (ν-(CH)), 2975 w, 2923 w, 2850 w, 2840 m, 2803 w, 1668 sh, 1654 vs, 1590 w, 1551 s, 1526 s, 1504 s, 1482 m, 1462 m, 1446 w, 1410 w, 1341 w, 1277 m, 1264 vs, 1199 vs, 1153 sh, 1139 vs, 1103 w, 1090 m, 1074 s, 1016 m, 954 m, 906 m, 806 w, 794 s, 783 w, 765 w, 741

(8) Maverick, A. W.; James, A. M.; Fan, H.; Isovitsch, R. A.; Fronczek, F. R. Paper presented at the 209th National Meeting of the American Chemical Society, Anaheim, CA, 1995; see Abstract INOR 465.
(9) Goel, S. C.; Kramer, K. S.; Chiang, M. Y.; Buhro, W. E. *Polyhedron* **1990**, *9*, 611.
(10) Young, V. L.; Cox, D. F.; Davis, M. E. *Chem. Mater.* **1993**, *5*, 1701.
(11) (a) Bertrand, J. A.; Kaplan, R. I. *Inorg. Chem.* **1966**, *5*, 489. (b) Funck, L. L.; Ortolano, T. R. *Inorg. Chem.* **1968**, *7*, 567.
(12) Holtzclaw, H. F.; Lintvedt, R. L.; Baumgarten, H. E.; Parker, R. G.; Bursey, M. M.; Rogerson, P. F. *J. Am. Chem. Soc.* **1969**, *91*, 3774.
(13) Morris, M. L.; Moshier, R. W.; Sievers, R. E. *Inorg. Chem.* **1963**, *2*, 411.
(14) Thornton, D. A. *Coord. Chem. Rev.* **1990**, *104*, 173.

Table 1. CHN Elemental Analytical Data for **4**−**11**

	% calcd			% found		
compd	C	H	N	C	H	N
4	26.75	1.68	2.60	26.85	1.82	2.62
5	31.02	2.60	2.41	31.07	2.67	2.40
6	32.31	2.88	2.35	32.33	3.03	2.41
7	31.02	2.60	2.41	31.02	2.63	2.45
8	30.66	2.73	2.23	30.76	2.74	2.30
9	31.55	3.61	3.34	31.11	3.59	3.21
10	30.13	3.09	3.90	30.14	3.09	3.80
11	30.53	2.83	2.54	30.63	2.44	2.63

Table 2. Thermal Data for the $Cu(hfacac)_2$ Complexes

	mp, °C	DSC, °C[a]	T_{subl}, °C[b]
1	98−99[11a]	82N, 100N, 254N	103.9
2	133−136[11b]	122N, 138N, 167N	103.8
3	205−206[7]	205N	152.5
4	154−155	154N, 169N	160.7
5	74−78	47N, 82N, 161N, 214X	143.0
6	139−142	147N, 184X, 252X	156.8
7	56−58	63N, 206X	164.5
8	121−123		dec
9	160−162 dec	142N, 169X, 192X	dec
10	194−195	200N, 206X, 214X	204.4
11	70−71	71N, 77N, 153N, 165N	138.4

[a] Peak temperatures; N = endothermic, X = exothermic. [b] Inflection points on mass-loss curves; sample weights 10.0−10.6 mg.

w, 669 vs, 646 w, 588 m, 578 w, 528 w; ^{19}F NMR (toluene-d_8) δ −63.6 ($\Delta\nu_{1/2}$ = 85 Hz) at 25 °C, −57.9 ($\Delta\nu_{1/2}$ = 150 Hz) at −90 °C.

Compound 11. *n*-$BuNH_2$ (0.30 mL, 3.0 mmol) was added to **1** (1.45 g, 3.04 mmol) in 50 mL of toluene with stirring. The green solution color deepened. After removal of the solvent in vacuum, the green solid was sublimed at 75−90 °C and 0.01 Torr, providing 78% **11**: mp 69.5−70.5 °C; IR (KBr pellet, 4000−400 cm^{-1}) ν 3331 w (ν_{as}(NH)), 3274 m (ν_s(NH)), 3147 w (ν(CH)), 2969 m, 2941 w, 2882 w, 1653 sh, 1645 vs, 1611 m, 1558 s, 1533 s, 1483 s, 1462 vs, 1357 w, 1342 w, 1258 vs, 1203 vs, 1154 sh, 1144 vs, 1112 w, 1100 w, 1088 w, 1035 w, 987 w, 948 w, 805 m, 800 m, 770 w, 743 w, 677 m, 671 m, 591 m, 579 w, 528 w.

Compound 14. Solid glycine (0.3068 g, 4.087 mmol) was added to a solution of **1** (1.951g, 4.085 mmol) in 125 mL of MeOH, and the suspension was stirred at room temperature overnight. A fine blue-violet precipitate was filtered off and dried in vacuum, giving 0.311 g (72%, based on eq 2) of **14.** Its IR spectrum compared well with the literature data.[15] All volatile components were removed from the filtrate, giving a green solid which, after washing with water and drying in air, yielded 56% unreacted **2**.

Results of elemental analyses for compounds **4**−**11** are listed in Table 1.

Thermal Analyses. Differential scanning calorimetry (DSC) was performed on a DuPont Instruments 910 differential scanning calorimeter under a flowing helium atmosphere (40 mL/min). The samples (6−10 mg) were crimped in aluminum pans inside a helium-filled glovebox, transferred to the DSC cell, and heated to 500 °C at 5 °C/min. The peak temperatures are reported in Table 2. Thermogravimetric mass spectral analyses (TGA-MS) were carried out on a DuPont Instruments 951 thermogravimetric analyzer (enclosed in a helium-filled glovebox) coupled to a VG Micromass PC Quadrupole Mass Spectrometer (QMS). Samples (mass of 10.0−10.6 mg) were heated under flowing helium (40 mL/min) on platinum pans to to 500 °C at 5 °C/min, and volatile products were delivered through a heated capillary to the QMS inlet. Sublimation temperatures are reported here as the inflection point on the TGA curve (Table 2).

Vacuum Pyrolyses of 8. Compound **8** (350 mg) in a Pyrex vial was placed in a pyrolytic tube connected by an O-ring joint to an NMR tube. The system was evacuated, and one end of the pyrolytic tube was inserted into a horizontal furnace while the NMR tube was cooled with liquid nitrogen. The temperature was ramped at 10 °C/min to a desired value (125, 200, or 400 °C) and then kept constant for 30 min. After the sample was cooled to room temperature, $CDCl_3$ was added by vacuum transfer and the NMR tube was flame-sealed. ^1H, ^{13}C, and ^{19}F NMR spectra established identities of the pyrolytic products. Hhfacac: ^1H δ 6.39 (1H, s, CH), 12.72 (1H, s, OH); ^{13}C δ 177.0 (q, $^2J_{CF}$ = 39 Hz, CO), 116.8 (q, $^1J_{CF}$ = 282 Hz, CF_3), 94.1 (s, CH); ^{19}F δ −76.9. CF_3COCH_3: ^1H δ 2.42 (s); ^{13}C δ 189.3 (q, $^2J_{CF}$ = 36 Hz, CO), 115.9 (q, $^1J_{CF}$ = 292 Hz, CF_3), 23.8 (s, $^1J_{CH}$ = 130.5 Hz, CH_3); ^{19}F δ −80.7. CF_3H: ^1H δ 6.50 (q, $^2J_{FH}$ = 79 Hz); ^{13}C not observed; ^{19}F δ −78.4 (d, $^2J_{FH}$ = 79 Hz).

Single-Crystal X-ray Diffraction Studies of 1·C_7H_8, 4, 10, and 9·0.5MeOH. The single crystals of **1**·C_7H_8 were grown from a toluene solution of **1** at −20 °C, while the crystals of **10** and **9**·0.5MeOH were obtained from methanol solutions at the same temperature. Vapor diffusion of $CHCl_3$ into the saturated methanol solution at room temperature gave single crystals of **4**.

Crystals (all of irregular habit) were affixed to the tip of a glass fiber using silicone grease and transferred to the goniostat, where they were cooled for characterization and data collection.[16] The crystals of **1**·C_7H_8 underwent an apparent phase transition and split when cooled below −110 °C. For handling of **1**·C_7H_8, standard inert-atmosphere techniques were used, while **4**, **10**, and **9**·0.5MeOH are air-stable and no special precautions were taken. Pertinent crystallographic data are presented in Table 3. Data were collected by the moving-crystal, moving-detector technique with fixed background counts at each extreme of the scan. Data were corrected for Lorentz and polarization effects, and equivalent data were averaged. The structures were solved by direct methods (MULTAN78 for **1**·C_7H_8 and **10**, SHELXTL for **4** and **9**·0.5MeOH) and Fourier techniques.

Three of the eight CF_3 groups in the asymmetric unit of **4** were found to be disordered as well as the carbon backbone of the ethanolamine ligand in one of the two independent molecules. Because it was not possible to distinguish reliably oxygen and nitrogen of ethanolamine from the electron density map, a chemical distinction between the two heteroatoms was employed; namely, the moiety bonded at a longer distance was assigned to the OH group and the one at a shorter distance to the amine.[17] No corrections were made for extinction.

A systematic search of reciprocal space of **9**·0.5MeOH located a set of data with symmetry and systematic absences corresponding to the monoclinic space groups $P2_1$ and $P2_1/m$. In this case, the space group choice is ambiguous. The structure can be solved and refined in both space groups with comparable final agreement indices. The final model in the noncentrosymmetric space group $P2_1$ has only small deviations from mirror symmetry but is fully ordered, whereas the final model in the centrosymmetric space group $P2_1/m$ has some disorder (see below). It is usually the case with an almost centrosymmetric structure that there is no well-defined global minimum for the least-squares process, but rather several similar local minima. The final parameters determined with a noncentrosymmetric model can therefore be deceiving, and at the least their esd's tend to be vastly underestimated. The centrosymmetric model represents an average structure, but the least-squares minimum is generally well-defined, and the esd's are therefore more reliable.[18] Because of these considerations, the structure was modeled in space group $P2_1/m$.

Results and Discussion

In spite of the considerable technological importance of our starting material, anhydrous $Cu(hfacac)_2$, **1**, its molecular structure has not been previously reported; therefore, we grew crystals suitable for X-ray diffraction experiments by sublimation. Despite an excellent appearance of the samples, our attempts to separate suitable single crystals from the cold finger failed owing to an extremely easy plastic deformation of the crystals. Crystallization of **1** from toluene provided the solvate **1**·C_7H_8 whose molecular structure is shown in Figure 1.

(15) Sen, D. N.; Mizushima, S.; Curran, C.; Quagliano, J. V. *J. Am. Chem. Soc.* **1955**, *77*, 211.

(16) For a general description of diffractometer and crystallographic procedures, see: Chisholm, M. H.; Folting, K.; Huffman, J. C.; Kirkpatrick, C. C. *Inorg. Chem.* **1984**, *23*, 1021.

(17) Orpen, A. G.; Brammer, L.; Allen, F. H.; Kennard, O.; Watson, D. G.; Taylor, R. *J. Chem. Soc., Dalton Trans.* **1989**, S1.

(18) Marsh, R. E. *Acta Crystallogr., Sect. B* **1986**, *42*, 193.

Table 3. Crystallographic Data for **1**·C_7H_8, **4**, **9**·0.5MeOH, and **10**

	1·C_7H_8	**4**	**9**·0.5MeOH	**10**
formula	$CuC_{17}H_{10}O_4F_{12}$	$CuC_{12}H_9O_5NF_{12}$	$CuC_{12}H_{17}O_6NF_6$·$0.5CH_3OH$	$Cu_2C_{18}H_{22}O_6N_2F_{12}$
fw	569.79	538.73	626.84	717.45
a, Å	6.510(6)	13.145(1)	10.075(4)	9.259(2)
b, Å	8.594(7)	13.418(1)	8.611(4)	12.011(3)
c, Å	18.478(15)	11.245(1)	19.259(9)	6.304(1)
α, deg	90	110.39(1)	90	91.19(1)
β, deg	90	99.12(1)	99.82(2)	106.66(1)
γ, deg	90	97.90(1)	90	74.83(1)
V, Å^3	1033.76	1795.36	1646.52	647.17
Z	2	4	4	1
space group	*pmnn* (No. 58)	$P\bar{1}$ (No. 2)	$P2_1/m$ (No. 11)	$P\bar{1}$ (No. 2)
T, °C	−103	−158	−168	−153
λ, Å	0.710 69	0.710 69	0.710 69	0.710 69
d_{calcd}, g cm^{-3}	1.831	1.993	2.529	1.841
μ, cm^{-1}	11.832	13.614	15.109	17.674
$R(F)^a$	0.0465	0.0477	0.0497	0.0570
$R_w(F)^b$	0.0466	0.1174[c]	0.0995[c]	0.0582
GOF	2.750	1.738	1.032	1.735

[a] $R(F) = \sum||F_o| - |F_c||/\sum|F_o|$. [b] $R_w(F) = [\sum w(|F_o| - |F_c|)^2/\sum w|F_o|^2]$ where $w = 1/\sigma^2(|F_o|)$. [c] $R_w(F^2) = [\sum w(|F_o^2| - |F_c^2|)^2/\sum w|F_o^2|^2]^{1/2}$.

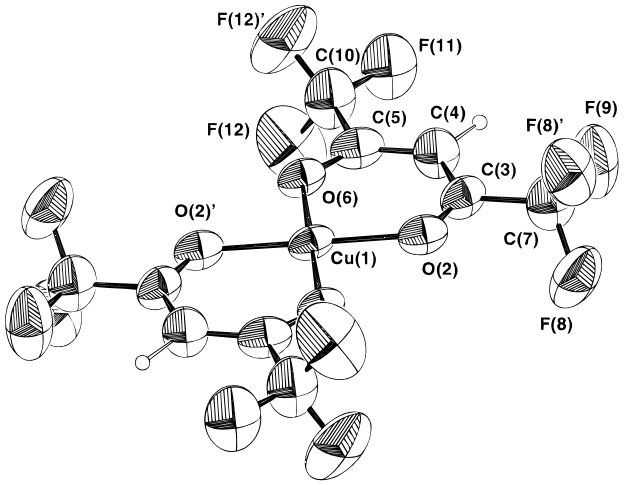

Figure 1. Molecular structure of Cu(hfacac)$_2$·C_7H_8. Thermal ellipsoids are drawn at the 50% probability level. Only symmetry-independent atoms are labeled.

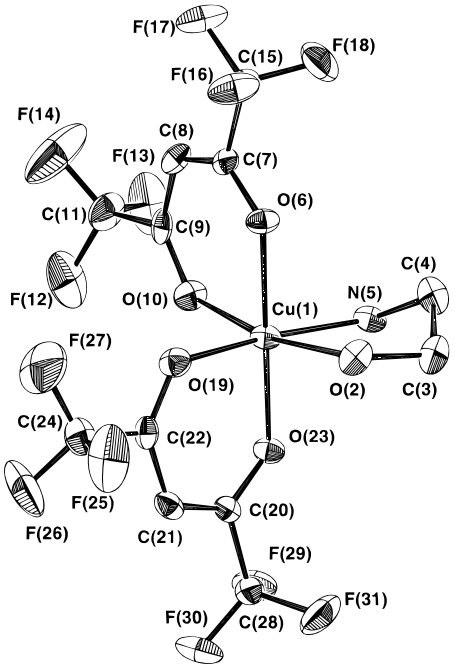

Figure 2. Molecular structure and atom-labeling scheme for Cu(hfacac)$_2$($NH_2CH_2CH_2OH$), **4**. Thermal ellipsoids are drawn at the 50% probability level. Atoms C(3) and C(4) were disordered in two sites. Only one of two independent molecules is shown.

The reaction of **1** with a series of ethanolamine derivatives (molar ratio 1:1) afforded several types of products. Ethanolamine, 2-(*n*-propylamino)ethanol, 2-(*tert*-butylamino)ethanol, 1-(dimethylamino)-2-propanol, and triethanolamine (in toluene/THF) coordinate to the copper center through both amino and alcohol groups, forming complexes **4**−**8**, respectively. Elemental analyses (Table 1) and the presence of the OH stretching band in the IR spectra of **4**−**8** support the proposed constitution. The molecular structure of **4** was established by X-ray diffraction and is depicted in Figure 2.

A substantially different reactivity pattern was found in reactions of **1** with triethanolamine (in MeOH) and 2-(dimethylamino)ethanol. Both reactants coordinate to the copper center through their nitrogen moieties. Moreover, the proton of their hydroxo group is transferred to one of the hfacac ligands which is thus displaced as Hhfacac with the formation of mixed diketonate−alkoxide complexes **9** and **10**, respectively. Sterically less demanding 2-(dimethylamino)ethanol allows for dimerization and formation of **10** (Figure 3), while bulkier triethanolamine, containing two additional hydroxo groups capable of coordinating to the copper center, preserves the monomeric nature of **9** (Figure 4).

As noted above, a surprisingly small change in reaction conditions led, in the case of triethanolamine, to the isolation of both adduct (**8**, in toluene/THF solvent) and mixed diketonate−alkoxide (**9**, in MeOH solvent) complexes. Furthermore, the proton transfer reaction and the loss of Hhfacac from **8** were initiated by an increase in temperature (eq 1). The transformation of **8** to **9** was followed by thermogravimetric methods. The first step (103−125 °C) on the TG mass-loss curve (Figure 5) corresponds to the elimination of the Hhfacac molecule from **8** (found 32.8%, theoretical 33.2%). In the pyrolytic decomposition experiment at 125 °C (see Experimental Section), the liberated ligand was trapped as the only volatile product, and ^{1}H, ^{13}C, and ^{19}F NMR spectroscopies confirmed its identity.

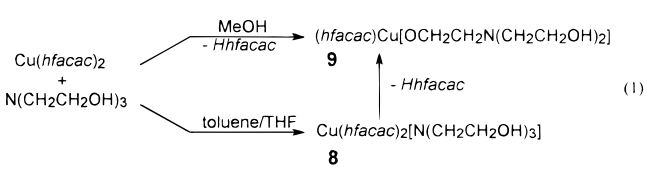

Apparently, the coordination of the amine nitrogen to the copper atom of **1** plays an important role in the course of formation of **9** and **10** as acidity of aliphatic alcohol protons is

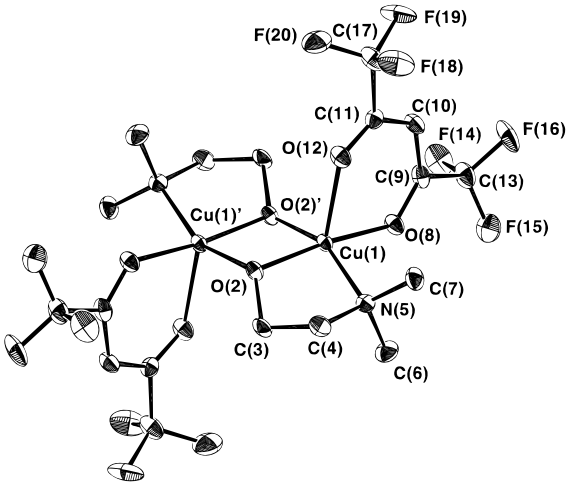

Figure 3. Molecular structure and atom-labeling scheme for $[Cu(hfacac)(OCH_2CH_2NMe_2)]_2$, **10**. Thermal ellipsoids are drawn at the 50% probability level. Unlabeled atoms are related to the labeled ones by an inversion center.

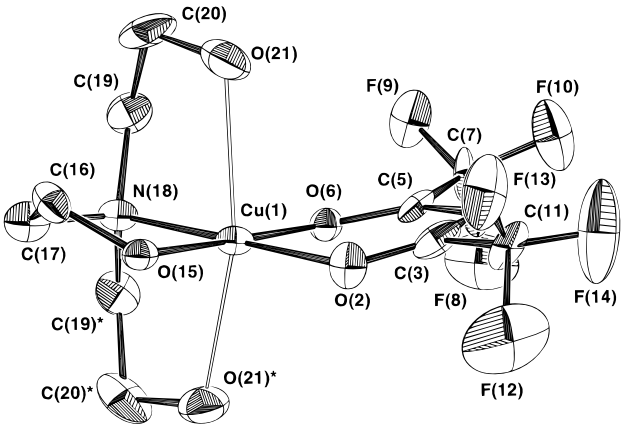

Figure 4. Molecular structure and atom-labeling scheme for one of the two crystallographically independent molecules of $Cu(Hfacac)[OCH_2CH_2N(CH_2CH_2OH)_2]\cdot MeOH$, **9**·MeOH. Thermal ellipsoids are drawn at the 50% probability level. Starred atoms are related by mirror symmetry to the corresponding unstarred ones. The disorder (mirror generated) counterparts of C(17), C(16), and the hfacac carbons and fluorines are omitted for clarity.

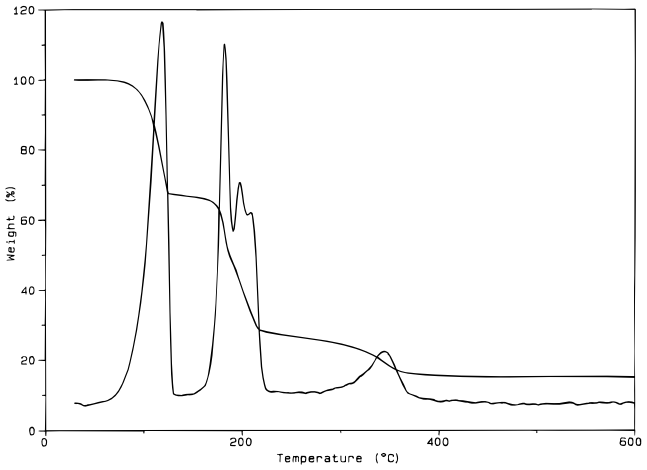

Figure 5. TG mass-loss curve and its first derivative for $Cu(hfacac)_2[N(CH_2CH_2OH)_3]$, **8**.

much smaller ($pK_a(H_2O) = 15$[19]) than the acidity of Hhfacac ($pK_a(H_2O) = 5.3$[20] -6.0[21]). This was underscored by observing no reaction in toluene at 95 °C between **1** and $(CF_3)_3COH$ whose acidity ($pK_a(H_2O) = 5.4$[22]) is comparable to that of Hhfacac. Therefore, we can speculate that the amine coordination causes a substantial weakening of at least some of the Cu−O (hfacac) bonds. This is supported by the observed lengthening of the Cu−O bonds in **3**,[7] **4**, **9**, and **10** (up to 2.25 Å) in comparison to the ones in **1** (1.91 Å). Associated with this bond lengthening may be an increase in the Brønsted basicity of the hfacac oxygen. To model increased acidity of the OH group, α-substituents in ethanolamine were replaced with an oxo group. The reaction of glycine with **1** proceeded with a complete displacement of both hfacac ligands (eq 2). Even when reactants were mixed in the 1:1 ratio, only the fully substituted product **14** and the unreacted **1** were isolated.

Table 4. ^1H NMR Data for **10** at Room Temperature in Varioius Solvents

solvent	δ, ppm	$\Delta\nu_{1/2}$, Hz	solvent	δ, ppm	$\Delta\nu_{1/2}$, Hz
toluene-d_8	106.5[a]	970	CD_2Cl_2	117.3[a]	930
	74.7[b]	550		81.4[b]	610
	70.8[c]	570		76.2[c]	700
$CDCl_3$	114.5[a]	67	acetone-d_6	117.1[a]	1090
	79.1[b]	30		82.6[b]	650
	74.7[c]	40		77.2[c]	680

[a] CH_2O (4H). [b] CH_3N (12H). [c] CH_2N (4H).

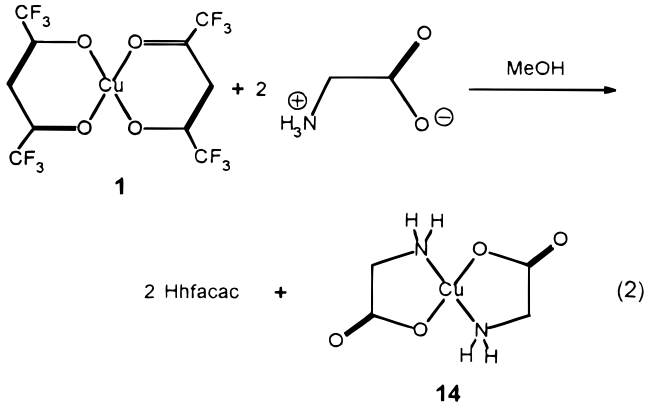

The persistence of the dimeric structure of **10** in solution was evidenced in its ^1H NMR spectrum. Dinuclear Cu^{2+} complexes with magnetic coupling between the two paramagnetic centers produce observable ^1H NMR spectra because of the presence of an effective electron relaxation mechanism.[23] Compound **10** displays three broad signals in the ratio 1:3:1 in the downfield region 70−117 ppm (Table 4). They can be tentatively assigned to the protons of the $Me_2NCH_2CH_2O$ ligands. The signal for the hfacac proton was not located. The ^{19}F NMR spectrum of **10** consists of a singlet at −63.6 ppm (half-width $\Delta\nu_{1/2} = 85$ Hz) which does not decoalesce upon cooling to −90 °C. Thus, the process that averages the two inequivalent CF_3 groups is very fast on the NMR time scale. The suggested mechanism of this interconversion is shown in Scheme 1 and involves a transition state with the trigonal-bipyramidal copper centers. The departure of the coordination geometry from the ideal square-pyramidal toward trigonal-bipyramidal was noted in the solid state structure of **10** (see "Structural Considerations" below). Upon addition of Hhfacac to the toluene-d_8 solution of **10** (4:1), the ^{19}F NMR signal shifted and broadened ($\delta(^{19}F) = -55$, $\Delta\nu_{1/2} = 5$ kHz). The position and the width of this signal are

(19) Rochester, C. H. In *The Chemistry of the Hydroxyl Group*; Patai, S., Ed.; J. Wiley & Sons: New York, 1971; Part 1, p 369.

(20) Reutov, O. A.; Beletskaya, I. P.; Butin, K. P. *CH-Acids*; Pergamon Press: New York, 1978; p 192.

(21) Shaikhutdinov, S. K.; Shupik, A. N.; Trukhan, E. M. *J. Chem. Soc., Faraday Trans.* **1993**, *89*, 3959.

(22) Willis, C. J. *Coord. Chem. Rev.* **1988**, *88*, 133.

(23) Satcher, J. H.; Balch, A. L. *Inorg. Chem.* **1995**, *34*, 3371.

Scheme 1

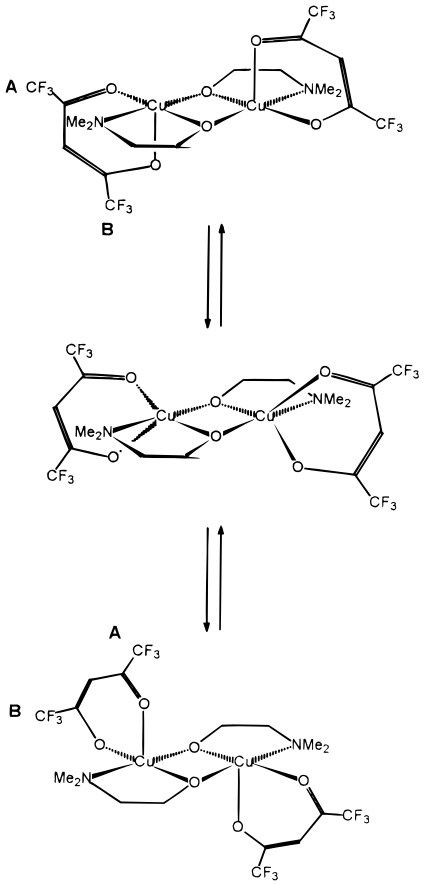

Scheme 2

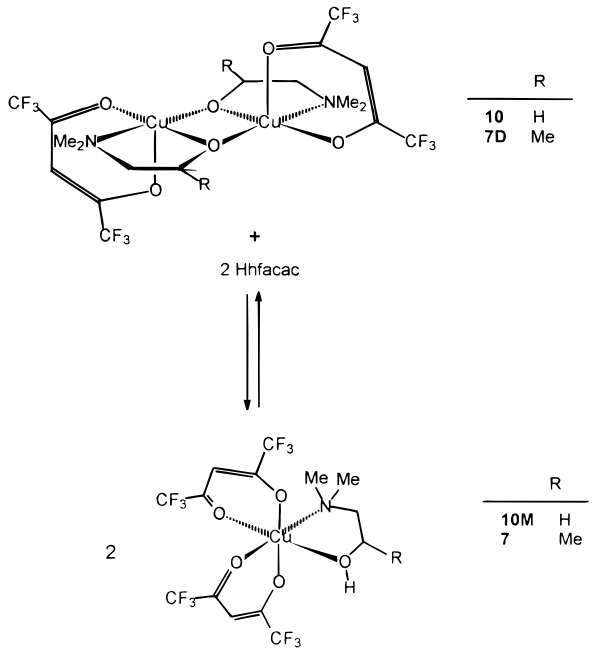

Table 5. ^{19}F NMR Data for Cu(hfacac)$_2$ Complexes in Toluene-d_8

	δ, ppm	$\Delta\nu_{1/2}$, Hz		δ, ppm	$\Delta\nu_{1/2}$, Hz
2	−41	6900	**10**	−63.6	85
4	−48	4010	**11**	−50	3400
7	−51	2975			

similar to those for the mononuclear complexes (Table 5) and indicate the presence of the mononuclear (**10M**) species formed from the dinuclear **10** according to Scheme 2. The reaction in the opposite direction was performed by heating the toluene-d_8 solution of **7** in a sealed NMR tube for several days to 100 °C.

Table 6. Selected Bond Distances (Å) and Bond Angles (deg) in **1**·C_7H_8, **4**, **10**, and **9**·MeOH

		1·C_7H_8	
Cu(1)−O(2)	1.908(7)	O(2)′−Cu(1)−O(6)	87.0(3)
Cu(1)−O(6)	1.914(6)	O(2)−Cu(1)−O(6)	93.0(3)
		4—Molecule A	
Cu(1)−O(2)	2.277(4)	O(6)−Cu(1)−O(10)	85.3(1)
Cu(1)−N(5)	2.003(4)	O(19)−Cu(1)−O(23)	90.0(2)
Cu(1)−O(6)	1.998(3)	O(2)−Cu(1)−N(5)	79.8(2)
Cu(1)−O(10)	2.254(4)	O(2)−Cu(1)−O(10)	169.1(2)
Cu(1)−O(19)	1.979(4)		
Cu(1)−O(23)	1.992(3)		
		4—Molecule B	
Cu(1)−O(2)′	2.355(4)	O(6)′−Cu(1)′−O(10)′	86.1(1)
Cu(1)′−N(5)′	1.992(4)	O(19)′−Cu(1)′−O(23)′	91.2(1)
Cu(1)′−O(6)′	1.994(3)	O(2)′−Cu(1)′−N(5)′	78.1(2)
Cu(1)′−O(10)′	2.256(4)	O(2)′−Cu(1)′−O(10)′	169.8(1)
Cu(1)′−O(19)′	1.963(4)		
Cu(1)′−O(23)′	1.971(3)		
		10	
Cu(1)−O(2)	1.919(4)	O(2)−Cu(1)−O(2)′	80.7(2)
Cu(1)−O(2)′	1.933(4)	O(8)−Cu(1)−O(12)	86.8(2)
Cu(1)−O(8)	1.980(4)	O(2)−Cu(1)−N(5)	85.8(2)
Cu(1)−O(12)	2.221(4)	O(2)−Cu(1)−O(8)	169.5(2)
Cu(1)−N(5)	2.020(5)	O(2)′−Cu(1)−N(5)	155.6(2)
		Cu(1)−O(2)−Cu(1)′	99.3(2)
		9·MeOH—Molecule A	
Cu(1)−O(15)	1.908(5)	O(2)−Cu(1)−O(6)	90.7(2)
Cu(1)−O(6)	1.970(5)	O(15)−Cu(1)−N(18)	87.1(2)
Cu(1)−O(2)	1.978(6)	N(18)−Cu(1)−O(21)	77.3(2)
Cu(1)−N(18)	2.035(7)	O(6)−Cu(1)−N(18)	89.5(2)
Cu(1)−O(21)	2.392(8)	O(2)−Cu(1)−O(15)	92.7(2)
		9·MeOH—Molecule B	
Cu(1)′−O(15)′	1.914(5)	O(2)′−Cu(1)′−O(6)′	91.4(2)
Cu(1)′−O(2)′	1.956(5)	O(15)′−Cu(1)′−N(18)′	87.5(2)
Cu(1)′−O(6)′	1.967(5)	N(18)′−Cu(1)′−O(21)′	78.0(2)
Cu(1)′−N(18)′	2.043(6)	O(6)′−Cu(1)′−N(18)′	90.7(2)
Cu(1)′−O(21)′	2.393(5)	O(2)′−Cu(1)′−O(15)′	90.4(2)

The broad signal of mononuclear **7** gradually diminished, and a new, relatively sharp signal at −62 ppm ($\Delta\nu_{1/2}$ = 285 Hz) appeared in the ^{19}F NMR spectrum, attesting to the formation of dinuclear **7D** (Scheme 2). Additionally, the presence of **7D** in the gas is consistent with mass spectroscopy experiments (see below).

For the purpose of a comparison of the physical properties of **3** and **4**, we also prepared Cu(hfacac)$_2$(NH$_2$-*n*-Bu), **11**, from the reaction between **1** and *n*-BuNH$_2$ (1:1) in MeOH. Its molecular structure should be similar to that of **3**.[7]

Structural Considerations. Cu(hfacac)$_2$·C$_7$H$_8$. The molecular structure of **1**·C_7H_8 is shown in Figure 1. The CuO_4 array and all carbon atoms are positioned on a crystallographic mirror plane, rendering the system ideally planar. The Cu−O average bond distance of 1.911(9) Å (Table 6) is very similar to the one obtained from electron diffraction experiments on gaseous **1** (1.919(8) Å).[24] A comparison of the bond lengths and bond angles of **1**·C_7H_8 with those of other copper β-diketonates,[25−30] shown in Table 7, reveals that the Cu−O bonds are slightly shorter and the O−Cu−O angle is wider (93.9(1)°) in **1**·C_7H_8 than in other Cu(hfacac) moieties. The molecules of **1** in the crystal are connected through short

(24) Thomas, B. G.; Morris, M. L.; Hilderbrandt, R. L. *J. Mol. Struct.* **1976**, *35*, 241.
(25) Starikova, Z. A.; Shugam, E. A. *Zh. Strukt. Khim.* **1969**, *10*, 267.
(26) Le Brun, P. C.; Lyon, W. D.; Kuska, H. A. *Inorg. Chem.* **1986**, *25*, 3106.
(27) Baidina, I. A.; Stabnikov, P. A.; Igumenov, I. K.; Borisov, S. B. *Koord. Khim.* **1984**, *10*, 1699.
(28) Baidina, I. A.; Gromilov, S. A. *Zh. Strukt. Khim.* **1991**, *32*, 395.
(29) Hon, P.; Pfluger, C. E.; Belford, R. L. *Inorg. Chem.* **1966**, *5*, 516.
(30) Watson, W. H.; Holley, W. W. *Croat. Chem. Acta* **1984**, *57*, 467.

Table 7. Comparison of the Cu−O Bond Lengths (Å) and Intra-Ring O−Cu−O Angles (deg) in $[R_AC(O)CHC(O)R_B]Cu[R_CC(O)CHC(O)R_D]$

R_A	R_B	R_C	R_D	Cu−O	O−Cu−O	ref
Me	Me	Me	Me	1.92(1)	95.0(4)	25
CF_3	CF_3	Me	Me	1.946(5)[a]	91.5(1)[a]	26
				1.887(5)[b]	94.7(1)[b]	
				1.940(8)[a]	90.8(2)[a]	27
				1.899(8)[b]	94.6(2)[b]	
CF_3	CF_3	CF_3	CF_3	1.911(9)	93.0(3)	this work
CF_3	CF_3	Me	Ph	1.952(4)[a]	91.0(1)[a]	28
				1.903(3)[c,d]	93.9(1)[c]	
				1.887(3)[c,e]		
Me	Ph	Me	Ph	1.931(5)[d]	93.0(2)	29
				1.914(5)[e]		
t-Bu	*t*-Bu	*t*-Bu	*t*-Bu	1.89(1)	93.2(3)	30

[a] hfacac side; average distance. [b] acac side; average distance. [c] bzac side. [d] Me side. [e] Ph side.

C(4)H···F contacts[31] of 2.62 Å and form a three-dimensional network containing channels along the *b* axis. This contrasts with the crystal structure of **2**, which forms dimeric units through

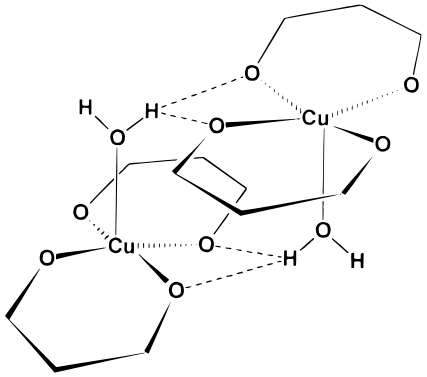

2

the hydrogen bonds, and moreover these dimers are connected into linear chains by weak CH···F bonds.[1]

Lying on the crystallographic mirror plane (and bisected by a C_2 axis) is a toluene molecule. This is seen as 16 half-weight peaks, which reveals that the disorder is not simply rotational (i.e., the methyl group on different ring carbons) but also translational (the ring center of gravity has perhaps four different locations), with partial overlap of certain disordered carbons. As a result, we cannot describe with certainty a single relationship between ring carbons and the CuO_4 moiety. However, the distance between these two planes is half the *a* axis length, or 3.26 Å. What can be seen from Figure 6 is the alignment of toluene molecules in channels parallel to the *b* axis. These channels can also be a source of partial loss of the lattice solvent content.

Cu(hfacac)$_2$(NH$_2$CH$_2$CH$_2$OH). The molecular structure of one of the two crystallographically-independent molecules of **4** is shown in Figure 2. Ethanolamine coordinates to copper through both O and N atoms. The coordination sphere around the copper center is a Jahn−Teller distorted octahedron elongated along the O(2)−Cu(1)−O(10) vector. The Cu(1)−N(5) bond distance is longer (average 1.998(6) Å) than the corresponding distance in **3** (1.933(6) Å),[7] in part due to the higher coordination number of the central atom. Similarly, the Cu(1)−O(2) bonds (2.277(4), 2.355(4) Å) are longer than the Cu−OH$_2$ distance (2.204(3) Å) in **2**[1] or the Cu−O (EtOH) distance (2.191(4) Å) in Cu(hfacac)$_2$(C$_2$H$_5$OH).[6] The Jahn−Teller distortion forces one of the hfacac ligands in each molecule of **4** to bind to copper in a very unsymmetrical fashion (average Cu−O(10) 2.255(6), Cu−O(6) 1.996(4) Å). An analogous situation was observed in Cu(hfacac)$_2$(bipy).[32] The second hfacac ligand in **4** is bonded symmetrically. The average Cu−O distances are 1.986(5) and 1.967(5) Å. There is weak hydrogen bonding between the alcohol group of ethanolamine and the oxygen of the hfacac ligand of the neighboring molecule (O(2)′···O(23) 2.77 Å).

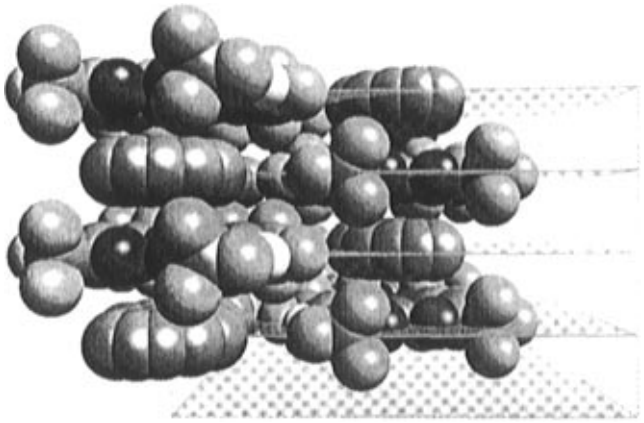

Figure 6. View of the crystal packing in three unit cells of Cu(hfacac)$_2$·C$_7$H$_8$ showing channels along the *b* axis (directed toward the viewer) filled with the solvent molecules. Trigonal pyramidal CF_3 groups indicate the Cu(hfacac)$_2$ molecules. The toluene molecules (e.g., upper right and lower left) are disordered around an axis perpendicular to their plane.

Cu(hfacac)[OCH$_2$CH$_2$N(CH$_2$CH$_2$OH)$_2$]·0.5MeOH. The asymmetric unit of **9** (Figure 4) contains two half-molecules, each residing on a crystallographic mirror plane. In the case of the second (primed) molecule (**B**), the hfacac ligand, the copper atom, and one nitrogen and one oxygen of the triethanolamine ligand are all located on the mirror plane. One ethyl arm of the triethanolamine and all of the fluorine atoms are disordered about the mirror. The other (unprimed) molecule (**A**) is similarly disordered, but in addition, its hfacac ligand is tilted out of the mirror plane at an angle of 15.4°. Only the hfacac oxygens are in the mirror plane; the rest of the ligand is disordered about the mirror. Despite the disorder, the hfacac is highly planar with no carbon or oxygen atom deviating by more than 0.019 Å from a least-squares plane. The coordination environment around copper is distorted octahedral with two long Cu−OH bonds (2.393(8) Å). The average Cu−O (hfacac) distance of 1.968(8) Å is similar to the corresponding distances of the symmetrically-bound hfacac ligand in **4**. The alkoxide O(15) and amine N(18) are bonded at average distances of 1.911(7) and 2.039(9) Å, respectively. A comparison with **12**[9] reveals that, while the amine bonds are similar in the two compounds (2.052(3) Å), the alkoxide bond in **12** is shorter (1.865(3) Å) than the one in **9**, as one would expect longer bonds for the compound with the higher coordination number of the central atom. For the amine bond in **12**, the decrease in the coordination number is offset by the presence of a stronger *trans* ligand. One triethanolamine OH group interacts with the alkoxide oxygen in the neighboring molecule (O(15)···O(21) 2.62 Å). Methanol of crystallization is involved in weak hydrogen bonding (shortest O···O contact 2.86 Å) to the triethanolamine alcohol group.

[Cu(hfacac)(OCH$_2$CH$_2$NMe$_2$)]$_2$. The molecular structure of the centrosymmetric dimer **10** is shown in Figure 3. The square-pyramidal geometry around the copper centers is distorted by

(31) The sum of van der Waals radii of H and F is 2.67 Å: Bondi, A. *J. Phys. Chem.* **1964**, *68*, 441.

(32) Veidis, M. V.; Schreiber, G. H.; Gough, T. E.; Palenik, G. J. *J. Am. Chem. Soc.* **1969**, *91*, 1859.

25% toward the trigonal bipyramid (using both the τ parameter[33] and the dihedral angle method[34]). The average Cu−O bond length in the $Cu_2(\mu\text{-}O)_2$ moiety (1.926(6) Å) is slightly shorter than the corresponding average distance (1.956(5) Å) in **15**.[35] The nonbonded Cu(1)−Cu(1′ distance is 2.936(1) Å. As

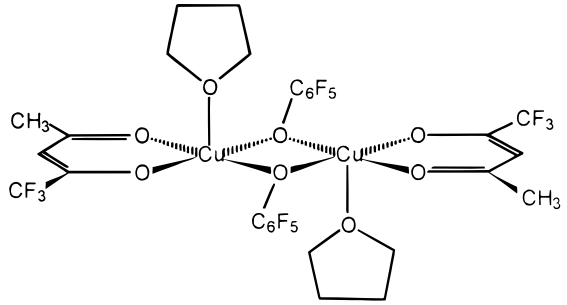

15

in **4**, the hfacac ligand has very asymmetric Cu−O distances (1.980(4) Å to the in-plane O(8) and 2.221(4) Å to the apical O(12)).

Thermal Behavior. To evaluate the utility of our series of compounds as precursors for CVD of copper, we examined their thermal characteristics such as melting points and sublimation temperatures by means of thermal gravimetric analysis (Table 2). Three compounds (**5**, **7**, and **11**) have lower melting points than the parent **1**. This may allow use of these precursors in the liquid state at conveniently low (60−80 °C) source temperatures. All prepared compounds, except **8** and **9**, sublime without decomposition at atmospheric pressure in the range 138−204 °C. Thermal decomposition of **8** was examined by the TGA-MS method (Figure 5). It shows a five-step reaction (inflections at 120, 182, 197, 212, and 346 °C) which leaves ultimately metallic copper at 700 °C (by XRD). The first decomposition step corresponds, as was noted above, to a clean elimination of the first Hhfacac molecule. That the second diketonate moiety is released and partially decomposed to CF_3H and CH_3COCF_3 during the following; a series of three closely spaced events was suggested on the basis of the observation of the fragments CF_3^+ (*m*/*z* 69), CF_2H^+ (*m*/*z* 51), CF_2^+ (*m*/*z* 50), CH_3CO^+ (*m*/*z* 43), and CH_3^+ (*m*/*z* 15) in the mass spectrum of the volatile effluent within the temperature range from 145 to 225 °C. This was further corroborated by identification of Hhfacac, CH_3COCF_3, and CF_3H in the trapped volatile products after the vacuum pyrolysis of **8** at 200 °C by ^1H, ^{13}C, and ^{19}F NMR spectroscopies (see Experimental Section).

In the final step, the decomposition of the triethanolamine ligand takes place (Figure 5), as no fluorine-containing fragments are observed in the effluent mass spectrum above 225 °C. The final sample weight was consistently 5% higher than expected for pure Cu, suggesting carbon or oxygen retention. The observation of CF_3^+ (*m*/*z* 69) and CF_2^+ (*m*/*z* 50) fragments in the mass spectrum of the volatile products during the first and second reaction steps attests to a removal of the hfacac ligand in the early stages of the process possibly by a proton transfer from the triethanolamine OH groups. Peaks at *m*/*z* 28, 31, and 44, ascribed to triethanolamine decomposition, are present in all three stages of the pyrolysis.

Mass Spectroscopic and CVD Studies. Gas phase reactivity of our potential precursors is relevant to their use in CVD reactions. Therefore we studied the mass spectra of **1**−**10** using electron impact (EI, 30 eV), chemical ionization (CI, CH_4), and fast atom bombardment (FAB) ionization modes. In the EI spectra, the molecular peak was observable only for **1** and **10**. Ethanolamine-containing fragments, such as Cu(hfacac)L^+, CuL_2^+, and CuL^+, were observed for **3**, **6**, **7**, and **11**. Moreover, **7** displays a peak at *m*/*z* 642 whose isotope pattern identifies it as $Cu_2(hfacac)_2(OCHMeCH_2NMe_2)^+$. This ion may arise from fragmentation of dinuclear **7D**, which in turn is being formed from **7** by the proton-transfer-initiated Hhfacac release and dimerization (Scheme 2). This is in concert with our observation of the transformation of **7** into **7D** in solution. Using milder ionization techniques, such as CI and FAB, dinuclear fragments $Cu_2(hfacac)_2(OCHR''CH_2NR'R)^+$ were observed for **7** (R = R′ = R″ = Me), **6** (R = *t*-Bu, R′ = R″ = H), **5** (R = *i*-Pr, R′ = R″ = H), and **4** (R = R′ = R″ = H). In the FAB spectra, these peaks have relatively high intensities (20−100%). We consider these facts to be compelling evidence for the transformation of mononuclear complexes to their dinuclear counterparts as shown in Scheme 2.

We conducted preliminary qualitative CVD experiments to evaluate the ability of our precursors to deposit metallic copper in the absence of an external reductant. Procedures and the CVD reactor employed in these depositions were described earlier.[1] Silicon and glass slides were used as substrates. Compounds **4** and **10** gave no deposit below 450 °C. At 500 °C, a black film containing Cu and Cu_2O (by XRD) was obtained. This negative outcome was expected for our model compound **11**, as it contains no alcohol group, but it was surprising in the case of **4**. On the other hand, successful formation of a copper-containing film was achieved at the lower temperature of 450 °C from dinuclear **10**. A substantially lower substrate temperature of 300 °C was sufficient in the case of **7**. This may indicate that secondary alcohols/alkoxides are better reductants for copper than their primary analogues.

Conclusions. In this work we demonstrated that amine-containing ligands can strongly bind to $Cu(hfacac)_2$ and form trigonal-pyramidal compounds such as **3** and **11**. If the ligands possess a second donor group, e.g. hydroxyl in ethanolamines, it will also coordinate to the copper center and form mononuclear six-coordinate complexes such as **4**−**7**. An interplay between electronic properties of the two moieties determines whether the reaction stops at this stage or continues by the proton transfer from the OH group to the hfacac ligand with the consequent release of Hhfacac (Scheme 2) and the formation of mono(diketonato)−alkoxide complexes. If the coordination needs of the copper atom are satisfied by additional donor groups, the complex remains mononuclear as was observed in the case of **9**. Another possible way to increase the central atom coordination number is dimerization, which was found for **10**. This sequence of events is suggested to be a part of the mechanism of the CVD process leading to films containing copper. Both **7** and **10** deposit copper (XRD) at 300 and 450 °C, respectively, attesting to the reducing ability of alcohols and alkoxides.

Acknowledgment. This work was supported by Department of Energy Grant DE-FG02-90ER45427 through the Midwest Superconductivity Consortium.

Supporting Information Available: Listings of crystallographic data, X-ray experimental details, fractional coordinates, and anisotropic thermal parameters (16 pages). Ordering information is given on any current masthead page.

IC960370H

(33) Addison, A. W.; Rao, T. N.; Reedijk, J.; van Rijn, J.; Verschoor, G. C. *J. Chem. Soc., Dalton Trans.* **1984**, 1349.
(34) (a) Muetterties, E. L.; Guggenberger, L. J. *J. Am. Chem. Soc.* **1974**, *96*, 1748. (b) Holmes, R. R.; Dieters, J. A. *J. Am. Chem. Soc.* **1977**, *99*, 3318.
(35) Bidell, W.; Shklover, V.; Berke, H. *Inorg. Chem.* **1992**, *31*, 5561.